remote sensing

MDPI

Article

A First Assessment of Canopy Cover Loss in Germany's Forests after the 2018–2020 Drought Years

Frank Thonfeld [1,*], Ursula Gessner [1], Stefanie Holzwarth [1], Jennifer Kriese [1], Emmanuel da Ponte [1], Juliane Huth [1] and Claudia Kuenzer [1,2]

[1] German Remote Sensing Data Center (DFD), German Aerospace Center (DLR), 82234 Wessling, Germany; ursula.gessner@dlr.de (U.G.); stefanie.holzwarth@dlr.de (S.H.); jennifer.kriese@dlr.de (J.K.); emmanuel.daponte@dlr.de (E.d.P.); juliane.huth@dlr.de (J.H.); claudia.kuenzer@dlr.de (C.K.)
[2] Institute of Geography and Geology, University of Wuerzburg, 97074 Wuerzburg, Germany
* Correspondence: frank.thonfeld@dlr.de

Abstract: Central Europe was hit by several unusually strong periods of drought and heat between 2018 and 2020. These droughts affected forest ecosystems. Cascading effects with bark beetle infestations in spruce stands were fatal to vast forest areas in Germany. We present the first assessment of canopy cover loss in Germany for the period of January 2018–April 2021. Our approach makes use of dense Sentinel-2 and Landsat-8 time-series data. We computed the disturbance index (DI) from the tasseled cap components brightness, greenness, and wetness. Using quantiles, we generated monthly DI composites and calculated anomalies in a reference period (2017). From the resulting map, we calculated the canopy cover loss statistics for administrative entities. Our results show a canopy cover loss of 501,000 ha for Germany, with large regional differences. The losses were largest in central Germany and reached up to two-thirds of coniferous forest loss in some districts. Our map has high spatial (10 m) and temporal (monthly) resolution and can be updated at any time.

Keywords: forest; canopy cover loss; drought; Sentinel-2; Landsat-8; disturbance index; time series

Citation: Thonfeld, F.; Gessner, U.; Holzwarth, S.; Kriese, J.; da Ponte, E.; Huth, J.; Kuenzer, C. A First Assessment of Canopy Cover Loss in Germany's Forests after the 2018–2020 Drought Years. *Remote Sens.* **2022**, *14*, 562. https://doi.org/10.3390/rs14030562

Academic Editors: María Teresa Lamelas and Darío Domingo

Received: 13 December 2021
Accepted: 21 January 2022
Published: 25 January 2022

1. Introduction

Vast areas of Central and Northern Europe experienced a pronounced drought in 2018 [1]. Germany, among other countries, was heavily affected [2,3]. In some parts of the country, exceptionally dry conditions continued into spring 2021. The effects of the 2018 drought had a strong impact on Central European forests, particularly in the Czech Republic and Germany [4,5]. The annual forest condition report published by the German Federal Ministry of Food and Agriculture (BMEL) revealed worsening crown conditions not only for the four dominant tree species in Germany, namely, spruce (25% of all trees), pine (23%), beech (16%) and oak (11%), but also for less abundant species [6]. Only 21% of the regularly surveyed trees do not show any sign of bad crown conditions [6]. While the overall trend of worsening crown conditions can be observed since the beginning of the record in 1984, the last three years show a dramatic increase in the share of trees in bad condition. Extensive droughts cause severe stress to trees, and there is general agreement that the recent drought years have a strong negative impact on crown conditions in Germany [5,6]. This is amplified by the specific situation in Germany, where forests are often located in hilly regions or on poor soils, and many trees are planted at the margins of their climatic niche [7]. Once stressed by drought, trees are often more susceptible to insect damage. While deciduous trees often have the potential to recover from insect infestations, the situation is different for coniferous trees. The European spruce bark beetle (*Ips typographus*) is one of the most damaging pest insects of spruce forests in Europe: successful infestation is typically fatal to trees [8]. Under normal conditions, bark beetles enter only freshly dead or stressed trees while they can bypass tree defenses through coordinated mass attacks during outbreaks [8,9]. In Central Europe, large amounts of

fresh deadwood often occur after windthrows, triggering bark beetle outbreaks [10–12]. However, drought and heat, among other stressors, can also facilitate outbreaks [13–16]. During the 2018–2020 droughts, bark beetle management in Germany had a strong focus on the prevention of outbreak expansion via massive salvage and sanitation logging in outbreak areas and their surroundings [8]. Even though the efficiency of these measures is being increasingly questioned [8,17], immense salvage logging took place in response to the 2018–2020 drought situation in the Czech Republic [18], Austria [19] and Germany [20]. However, the numbers provided are mainly based on statistical sampling and are not spatially explicit [21]. Besides, the temporal development can only be traced via the annual tree crown assessments at yearly intervals [6]. Examples of typical canopy cover loss areas in the 2018–2020 droughts are shown in Figure 1. Large-scale clear-cut gaps in spruce monocultures are often bordered by recently infested trees that are not yet removed. Standing dead trees and small groups or individuals of standing live trees are often left in the clear-cut areas, usually trees from less abundant tree species. This is one option to increase the amount of deadwood, which increases species abundance and richness and thus has a positive effect on biodiversity [22], which is strongly interlinked with the various ecosystem services that forests provide [23]. Information about canopy cover loss and forest condition in general is important, not only as it needs to be reported to the public but also because German forests fulfill a wide range of ecosystem services [7]. For this reason, forests are observed not only by many stakeholders with diverse interests but also by people who acknowledge the importance of forests for their recreational potential.

Figure 1. Photographs of typical drought- and bark beetle-affected areas in spruce forests with large-scale clear-cuts due to salvage logging, standing dead trees and small groups or individuals of standing live trees (usually of less common species, such as fir or larch). All photos were taken by F. Thonfeld.

Remote sensing has proven to be valuable in detecting forest changes, particularly stand-replacing changes [24–29]. While the current focus is on satellite-based near-real-time alerting of changes in the tropical moist forests of Asia, Africa and South America [30,31], recent research also considers temperate forests. Of particular interest are the changes in response to storm events [32] or insect pests [18,19,33–35]; the European Forest Fire Information System (EFFIS) has already been operating a near-real-time alerting system since 2000 [36]. Generally, canopy cover loss alerts indicate likely changes in near-real-time, often with some measure of confidence [30,31], whereas annual change maps, such as the global forest change product of the University of Maryland [37], show high confidence with

regard to the detected changes actually being real changes on the ground. However, the latter typically use annual best-pixel composites [38–40] or temporal metrics [41–43] that lead to some ambiguity in correctly assigning a change to a particular year, as images taken under optimal conditions are typically weighted more heavily than winter acquisitions. Hence, changes happening late in a particular year are likely to be attributed to the next year.

Silvicultural practice in Germany avoids large-scale clear-cutting. The common harvest practice of selective logging is difficult to monitor with medium spatial resolution satellites such as Landsat or Sentinel-2, the latter operating only as of 2015. Consequently, in the past, scientific literature on forest disturbance in Germany had a focus on the early detection of insect pests, such as bark beetles [44,45], or windthrow detection [32,46,47], both with a variety of sensors [7], and did not consider logging. Even though early detection of bark beetle infestation [18,33] and the assessment of forest damage and other threats to forest health [48–50] became increasingly important in Central Europe over the past few years, to our knowledge, there is currently no comprehensive, spatially explicit assessment of stand-replacing clear-cuts and canopy cover loss in Germany. Earth-observation methods are not yet implemented in regular reporting at the national level [51], even though many agencies at federal or state levels run their own remote-sensing labs and use Earth-observation technologies on local to regional scales. The recent drought and the associated forest damage require measures other than systematic field sampling to obtain a holistic picture of the losses.

This article demonstrates an efficient method for mapping canopy cover loss in temperate Central European forests with high spatial (10 m) and temporal (monthly) resolution. We present the first spatially explicit assessment of the tree-loss areas in response to the 2018–2020 droughts in Germany. To achieve this goal, we used time-series Sentinel-2 and Landsat 8 data, and a spectral index largely insensitive to illumination conditions—the disturbance index (DI) [52]. The dense time series was aggregated to monthly composites, thereby removing outliers. From the monthly time series, we computed anomalies with respect to a reference period and applied simple thresholding to separate clear-cuts and dead trees from healthy and stressed forest stands. We identified changes persisting over the monitoring period, determined canopy cover loss dates on a per-pixel scale, and aggregated the results to different administrative levels. While existing annual crown condition assessments are a valuable source to identify general (long-term) forest health developments, the spatially explicit mapping of canopy cover loss is still missing in Germany. We aim to support forest management and scientific understanding with this first assessment of canopy cover loss after the 2018–2020 drought years.

The objective of this article is to introduce this new product, to describe how it is generated, and to demonstrate our first results.

2. Materials and Methods

2.1. Data and Pre-Processing

In the presented approach, we used all Sentinel-2 and Landsat-8 data since 2017 available via the Google Earth Engine (GEE) [53]. We did not exploit Landsat-7, due to the known orbit shift at the end of its lifetime [54] and because of the SLC-off effects, i.e., the failure of the scan line corrector in May 2003 that resulted in stripe-like gaps in the acquired images [55]. The Sentinel-2 level 2 surface reflectance dataset from GEE is available from 28 March 2017 onward and is composed of data downloaded from Sci-Hub and processed using sen2cor [56]. Sentinel-2 is a constellation of two satellites, Sentinel-2 A and B, each with a repetition rate of ten days. The combined dataset has a temporal resolution of two to three days at mid-latitudes. However, Sentinel-2B was only launched in March 2017, and the first scene over Germany that is available from GEE is from December 2017. In Table 1, it can be seen that the number of scenes is lowest in 2017 and is far higher in the following years. The Landsat-8 level 2 dataset available from GEE is composed of surface reflectance data processed using the land surface reflectance code (LaSRC) [57]. The repetition rate of Landsat-8 alone is 16 days, so the combined dataset of Sentinel-2 and Landsat-8 can result

in daily coverage or even in two acquisitions on the same day. The number of datasets available over Germany is shown in Table 1.

Table 1. The number of datasets of Sentinel-2 and Landsat-8 with less than 80% cloud cover, available for Germany in the Google Earth Engine (GEE) between January 2017 and April 2021. Numbers in brackets indicate all available datasets in GEE, irrespective of cloud cover.

Year	Sentinel-2	Landsat-8	Total
2017	2087 (4221)	492 (635)	2579 (4856)
2018	6921 (11,801)	579 (707)	7500 (12,508)
2019	6567 (12,049)	535 (661)	7102 (12,710)
2020	7067 (12,035)	534 (648)	7601 (12,683)
2021	2043 (3948)	157 (173)	2200 (4121)
Total	24,685 (44,054)	2297 (2824)	26,982 (46,878)

We applied a comprehensive preprocessing scheme in order to reduce the impact of cloud-contaminated pixels or other undesired artifacts as effectively as possible. Therefore, we applied conservative cloud masks to the individual Sentinel-2 and Landsat-8 collections and removed all acquisitions with more than 80% cloud coverage. For Sentinel-2, we made use of the GEE cloud probability product created with the Sentinel-2 cloud detector library (https://github.com/sentinel-hub/sentinel2-cloud-detector (accessed on 10 December 2021)), available as a separate image collection. The cloud masking procedure for Sentinel-2 also corrects parallax effects [58]. For Landsat-8, we used the Fmask output [59,60] to remove clouds and cloud shadows. From both sensors, we then selected the blue, green, red, near-infrared and the two shortwave-infrared bands and combined the two datasets into one collection. From the images of this collection, we calculated the normalized difference snow index (NDSI) [61] and the S3 snow index [62]. A final snow mask was computed by thresholding both indices (https://github.com/NASA-DEVELOP/ASIT (accessed on 10 December 2021)). This mask was used to exclude snow-covered pixels, which is essential since vast forested areas in Germany are frequently snow-covered during the winter. For each image, we computed the normalized difference vegetation index (NDVI) [63], and the tasseled cap (TC) components brightness, greenness, and wetness [64,65], using the formula for surface reflectance data [66]. Furthermore, we computed the disturbance index (DI), a feature based on TC indices that allow for the characterization of forests and forest disturbances [52]. DI differentiates between forest and disturbed (or non-forested) areas. In its original definition, the TC features brightness, greenness, and wetness are re-scaled to their standard deviation above or below each scene's mean values for forests (Equation (1)):

$$\begin{aligned} B_r &= \left(B - B_\mu\right)/B_\sigma \\ G_r &= \left(G - G_\mu\right)/G_\sigma \\ W_r &= \left(W - W_\mu\right)/W_\sigma \end{aligned} \quad (1)$$

where B_r, G_r and W_r are rescaled brightness, greenness and wetness; B_μ, G_μ and W_μ are the mean forest brightness, greenness and wetness; and B_σ, G_σ and W_σ are the standard deviations of forest brightness, greenness and wetness. Mean and standard deviations are derived from a reference population representative of the forest pixels in the scene [52]. The reference population in our case was all cloud-free forest pixels. However, to account for the seasonality of deciduous trees, we calculated the DI separately for deciduous and coniferous forests. As we assumed high proportions of forest pixels being disturbed in some scenes, we considered only pixels with an NDVI higher than 0.5 for the DI calculation of coniferous forest pixels. This criterion is not applicable to deciduous forests because healthy and disturbed deciduous trees are not distinguishable in winter. In this study, a forest mask was derived by combining the VEG_02 layer of the digital landscape model for Germany at a 1:250,000 scale (DLM250) [67] and the European-wide 2015 forest-type layer of the Copernicus Land Monitoring Service [68].

The DLM250 VEG_02 layer contains all German forest areas, including dedicated infrastructure such as service roads, as well as cleared and unstocked areas, but it does not differentiate between forest types. The Copernicus 2015 forest-type layer is based on Earth-observation data and has a spatial resolution of 20 m. It differentiates between deciduous and coniferous trees and contains all tree-covered areas, including those in urban areas, parks or along roads, that are not necessarily a part of forest land use. Hence, combining the two products reduces the official forest area to the stocked forest area. By using the 2015 forest layer rather than the more recent 2018 layer, we ensure that we have data for conditions prior to the recent changes since 2018. Images with fewer than 100 forest pixels were excluded from further analysis since scaling with only a few samples might bias the DI calculation.

The DI is finally derived by combining the rescaled TC features [52] (Equation (2)):

$$\mathrm{DI} = B_r - (G_r + W_r) \quad (2)$$

DI is not sensitive to within-scene illumination effects and separates disturbed forest areas very well from undisturbed forest areas. Moreover, it is only slightly affected by seasonal variation compared to the TC components and other TC-related indices [69].

A major problem of optical remote-sensing data analyses of dense time series is artifacts due to undetected clouds, cloud shadows, or snow cover. These observations occur as outliers that need to be cleaned. For this purpose, we filtered the per-pixel DI time series using a running median filter with a moving window size of thirty days.

2.2. Canopy Cover Loss Detection

We used the median DI of all Sentinel-2 and Landsat-8 observations in 2017 as a reference, representing conditions before the recent canopy cover loss induced by the droughts in 2018 in Central Europe. To detect canopy cover loss at a monthly resolution, we calculated the 10th percentiles of DI for each month of the observation period, starting in January 2018, and computed monthly differences of these monthly percentiles to the median DI 2017 reference. The monthly 10th percentile was chosen to reduce the sensitivity toward remaining clouds and similar artifacts. Figure 2 shows the number of monthly percentile composites available over the observation period. It can be seen that low mountain ranges and alpine areas have some gaps, due to persistent cloud cover or snow during winter. In the next step, we applied a fixed threshold t to the monthly difference layers to separate clear-cut areas and dead trees from living trees. We found a default value of t = 2 to be appropriate. Figure 3 exemplifies the major steps of data processing, including median smoothing, computation of monthly percentiles, and application of a threshold to detect canopy cover loss.

Deciduous trees often show high DI values in leaf-off conditions, which makes the winter detection of canopy cover loss ambiguous. During the last month of the observation period, April 2021, the deciduous trees were still senescent. The leaf-off situation can cause the false detection of changes. Therefore, we removed all detected canopy cover losses recorded in deciduous forests during the final winter months (November 2020–April 2021) as a post-processing step to obtain a realistic estimate. The application of the threshold to each monthly difference image resulted in a binary per-pixel time series, where 1 denotes detected tree-loss, usually a clear-cut area and hereafter called a hit, and 0 indicates that no clear-cuts or dead trees were detected. From this time series, several properties can be computed that determine the date of canopy cover loss, e.g., the first date of detected canopy cover loss, the start of a period of n consecutive hits, or the start of the last uninterrupted period of hits that persisted until the end of the observation period. We define as the date of canopy cover loss the point when two consecutive hits were detected for the first time in a time series, given that hits were also detected for this particular pixel at the end of the observation period. The workflow diagram is presented in Figure 4. Figure 5 shows an exemplary subset of a forest area during the reference period in 2017, in comparison to the

situation at the end of the observation period in April 2021, the respective difference image and the resulting canopy cover loss areas.

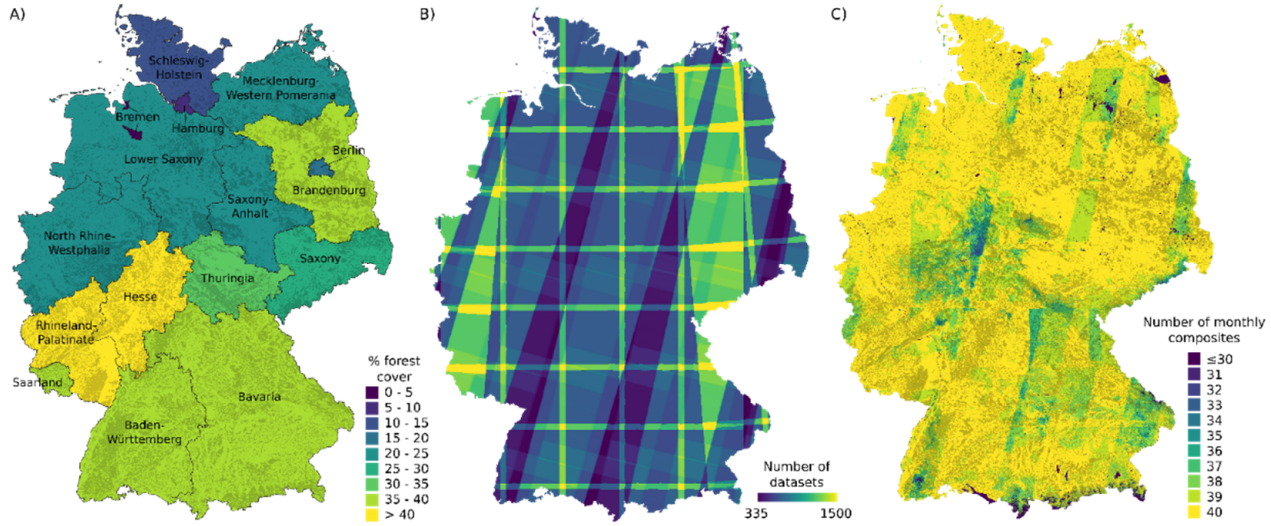

Figure 2. Forest cover per federal state: (**A**) the number of all Sentinel-2 and Landsat-8 datasets from January 2017–April 2021 over Germany; (**B**) the number of monthly Sentinel-2 and Landsat-8 percentile composites per pixel after pre-processing from January 2018–April 2021; (**C**) forest areas in the background of (**A**) and (**C**).

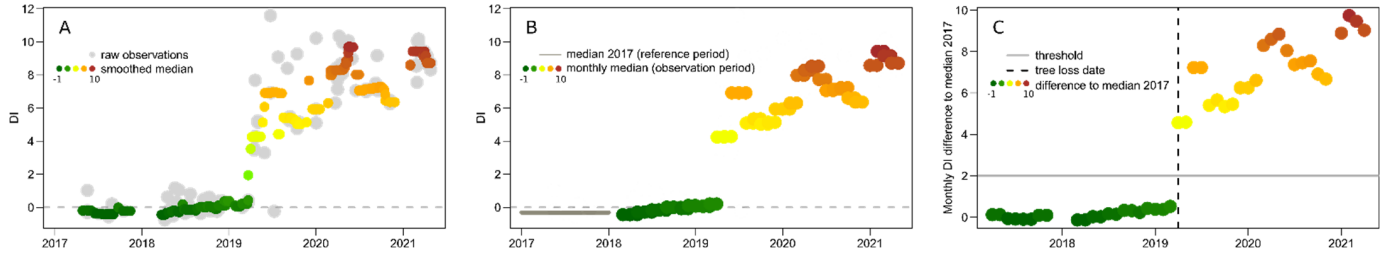

Figure 3. Major steps of the data processing exemplified at a disturbance index (DI) time series of a single pixel in a spruce forest in Southern Thuringia that became infested by bark beetle in 2018 and was cleared in April 2019. Processing includes median smoothing (**A**), computation of annual median for the reference period (2017) and monthly percentiles for the observation period (2018-April 2021) (**B**), and application of a threshold on the anomalies between monthly DI percentiles and the reference median to detect canopy cover loss (**C**).

To quantify the area affected by tree mortality and canopy cover loss, we computed statistics at various spatial entities, including hexagons, district level ("Landkreis") and federal state level ("Bundesland"). The hexagons have an in-circle diameter of 10 km, corresponding to an area of approx. 87 km^2. Federal state-level statistics address the scale at which forest condition is reported to the government. The district-level statistics are important to highlight regional differences, while the hexagons, representing an equal size reference, are useful to demonstrate local differences without bias. We derived the statistics from pixel counts since it is impossible to properly estimate the statistics based on samples, due to unavailable reference information at monthly resolution. All derived statistics are in relation to the respective forest type, i.e., coniferous forest or deciduous forest, or both in case all forest types are addressed.

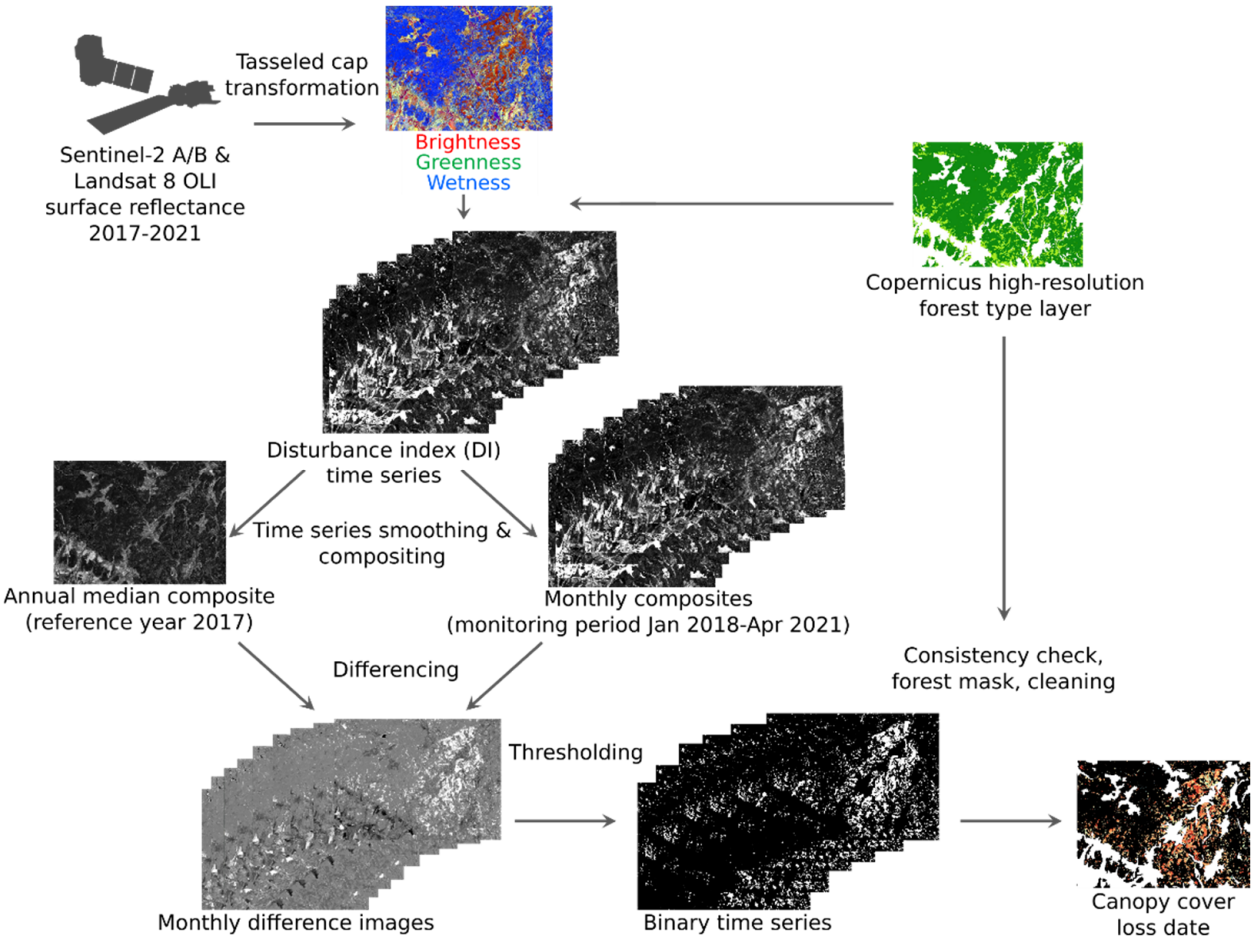

Figure 4. Workflow overview for the retrieval of the canopy cover loss dates per pixel.

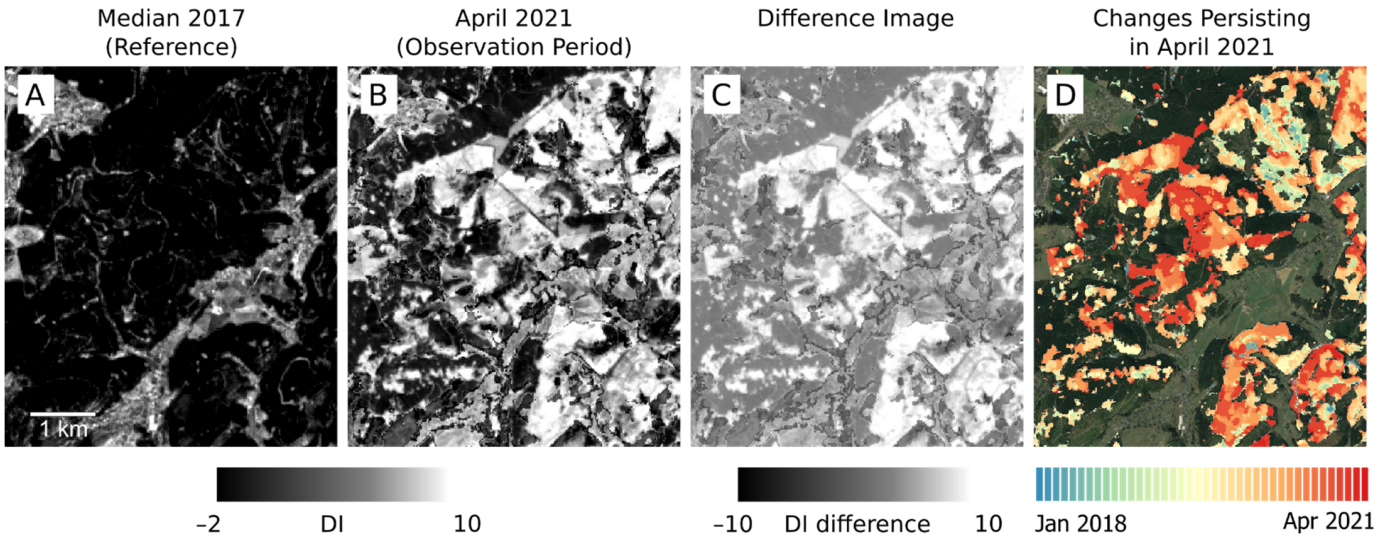

Figure 5. Disturbance index (DI) for the reference period (median 2017, **A**), DI for April 2021 (**B**), the difference of A and B (**C**), and the canopy cover loss mask, color-coded with the date of the canopy cover loss, overlaid on the Google Earth background image (**D**). Example from South Thuringia.

2.3. Validation

We validated the canopy cover loss product using optical satellite data and Google Earth high-resolution imagery. We generated three strata, with a total of 1538 sample

points. We allocated 1015 sample points to the stratum "canopy cover loss", whereby about 25 points were allocated to each month of the monitoring period, hence 40 months were included from January 2018 to April 2021. This allows us to have a good estimate of the false detection rate (commission error). We computed a three-pixel-wide buffer around the canopy cover loss areas and allocated 250 sample points in this buffer zone to target omission errors, which are more likely to occur in spatial proximity to existing canopy cover loss areas [70]. Additionally, we allocated 273 sample points to the stratum "intact forest", which excludes the buffer zone.

We checked each of the sample locations for canopy cover loss and dead trees, respectively, by visually examining corresponding Google Earth imagery for the same time period, available for most of the sample points. This was accompanied by the visual comparison of Sentinel-2 median composites, taken in summer 2017 as the initial condition, and in summer 2021 after the observation period (May–October 2021) as the final condition to validate samples without recent high-resolution images. While larger clear-cut areas can be easily detected, the identification of single dead or logged trees by visual interpretation is ambiguous. Therefore, we did not validate very small areas with three pixels of canopy cover loss or less. However, the vast majority of the detected canopy cover loss areas are significantly larger.

Validation of the temporal accuracy is amplified by the lack of appropriate data for most of the areas and most of the causes of tree mortality. The dying of the trees, the logging and their removal can take a certain time; therefore, the definition of tree death in response to droughts [71] and, hence, the timing of canopy cover losses are ambiguous. There is evidence that the separation of standing dead (spruce) trees and live trees, as well as non-forest, is possible [72], even though the process of change in spruce trees as they are dying is a gradient with several stages, such as green, red, and gray attack [17]. Generally, it is difficult to define exactly when a tree is dead [71,73,74]. We map canopy cover loss as the date when trees are without photosynthetic activity, or when forests are cleared. The latter includes salvation and sanitary logging and forest harvest. In case of storm events and fires, canopy cover loss can be directly associated with a particular date. Even then, it can take some time before cloud-free situations allow for the acquisition of optical data. We evaluated the recorded dates of some known fires that were captured during the observation period.

3. Results

Our results reveal that between January 2018 and April 2021, about 501,361 ha of forest in Germany were either cleared or left with dead standing trees, corresponding to 4.9% of the total forest area. Hence, this figure also includes dead trees that were not yet logged (Figure 6). Uncertainty exists regarding the canopy cover loss areas computed for the winter months at the end of the monitoring period (November 2020–April 2021). During this time, snow cover and frequent cloud cover limited the number of available observations. In addition, the phenology of deciduous trees in mixed forests can cause the overestimation of canopy cover loss. This is leveled out with summer detections of canopy cover loss and, hence, is only relevant for the last winter at the end of the monitoring period. Therefore, we consider all canopy cover losses detected between January 2018 and October 2020 to be reliable. This time frame accounts for 380,000 ha of canopy cover loss. Uncertainty is higher for the canopy cover loss areas detected during the last winter after October 2020, since more recent summer images would be needed to confirm or reject the detection. The area detected as canopy cover loss in winter 2020/2021 accounts for about 122,000 ha. The winter losses in the 2018/2019 and 2019/2020 winter seasons were 58,000 ha and 87,000 ha, respectively.

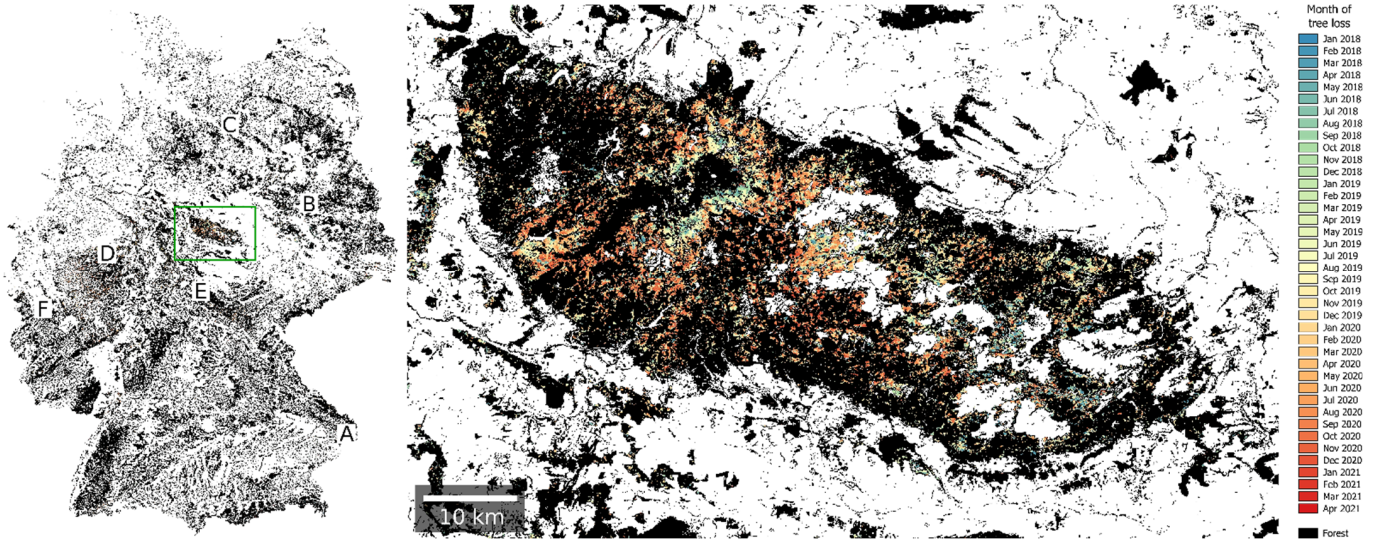

Figure 6. Canopy cover loss map for January 2018–April 2021 for Germany (left). One of the most severely affected regions is the Harz mountain range (right). Letters A-F indicate the locations of the examples shown in Figure 7.

Examples of large-scale canopy cover losses all over Germany are given in Figure 7. These examples comprise windthrow areas (Figure 7a,e), canopy cover loss due to fire events (Figure 7b,c), and clear-cuts (Figure 7d,–f). In windthrow areas, fallen trees are usually quickly removed but healthy trees are left standing. Therefore, windthrow areas are usually not entirely cleared.

Management after fire events sometimes includes the removal of dead trees. Occasionally, they are left standing to allow for natural regeneration. Dead spruce trees are usually removed to prevent further bark-beetle infestation. However, only limited forestry management is applied in national parks such as the Harz National Park or the Bavarian Forest National Park, and dead trees are often left standing.

In 2018, the canopy cover loss area was still rather low as it took some time for the trees to die in response to the heavy 2018 drought. Most of the cleared areas seen in early 2018 are likely the result of the removal of windthrown trees in the aftermath of the 2017 summer storms (e.g., near Passau in Bavaria, southeast Germany, Figure 7a) and 2018 winter storms such as "Friederike" (e.g., in northern and eastern Germany). However, drought-induced mortality in beech and spruce trees had already started in 2018 [75]. Canopy cover loss was accelerated by bark beetle infestation in spruce trees, which started in 2018 and continued in several outbreak phases until 2021. Salvage logging as a radical management strategy had already started in 2018 in some federal states, such as Saxony-Anhalt, but accelerated through 2019 and 2020, particularly in Hesse and North Rhine-Westphalia. Consequently, the spatial pattern of canopy cover loss changed from larger areas in eastern and southeastern Germany in 2018 to dominant changes in central and western Germany in 2019, 2020 and 2021 (Figure 8). Considering all forest types, canopy cover loss was evident throughout Germany, even though northern and southern Germany were less affected than central Germany (Figure 8). Central western and eastern Germany were most heavily affected with regard to forest loss in coniferous forests. In a belt ranging from the western to the eastern borders of the country, a large share of the coniferous forests was cleared or dead, in some areas by more than three-quarters.

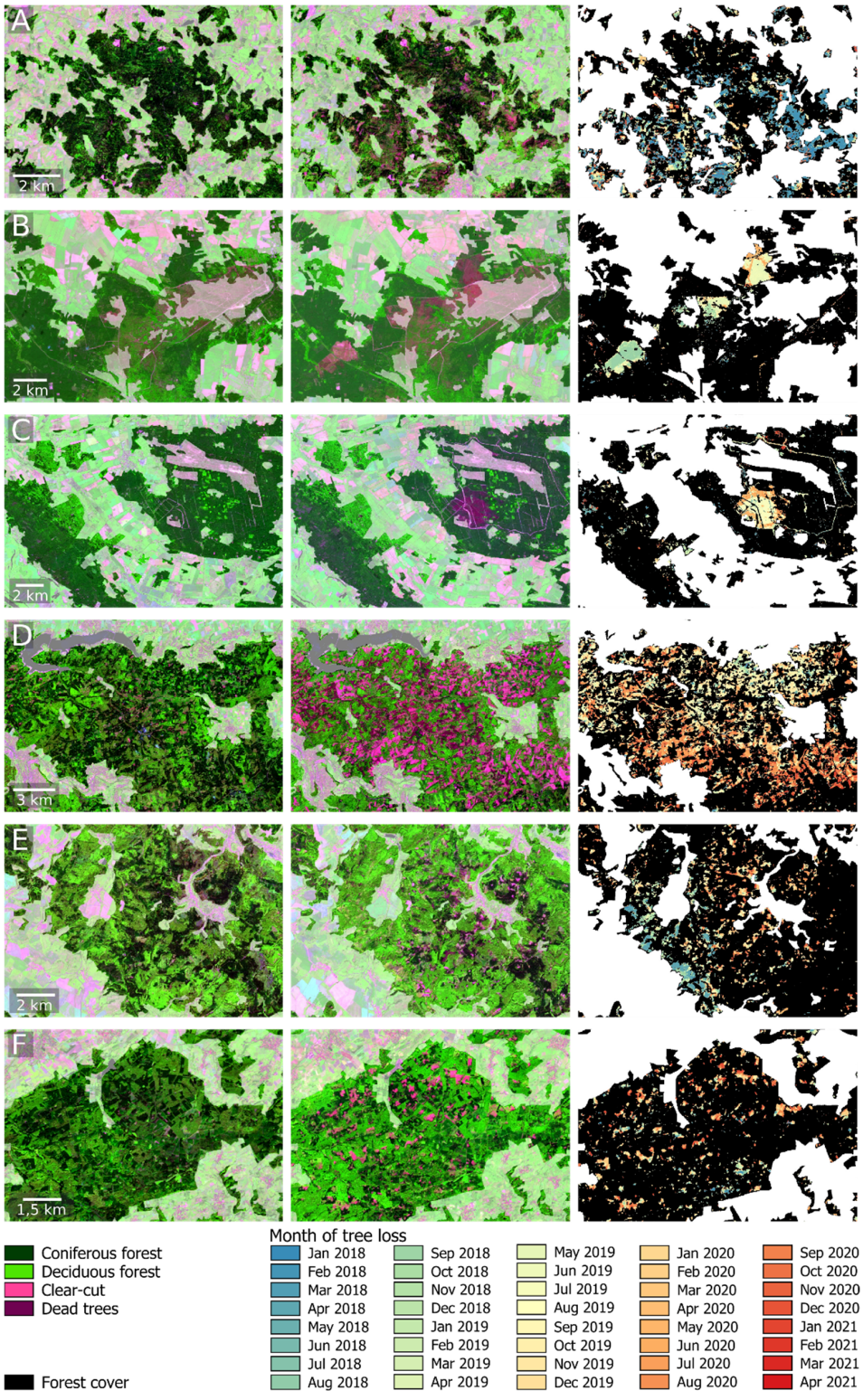

Figure 7. Examples of the situation in 2017 (median April–October, left column) compared to 2021 (median May–October, center column) and the detected canopy cover loss dates (right column): (**A**) storm damage near Hauzenberg, Bavaria, (**B**) fire scars near Treuenbrietzen, Brandenburg, (**C**) fire scars near Lübtheen, Mecklenburg-Western Pomerania, (**D**) salvage logging near Arnsberg, North Rhine-Westphalia, (**E**) storm damage and salvage logging near Ruhla, Thuringia, and (**F**) salvage logging in the northern Eifel region, North Rhine-Westphalia. False-color composites with RGB = SWIR-NIR-RED. The location of the displayed subsets is shown in Figure 6 (left panel).

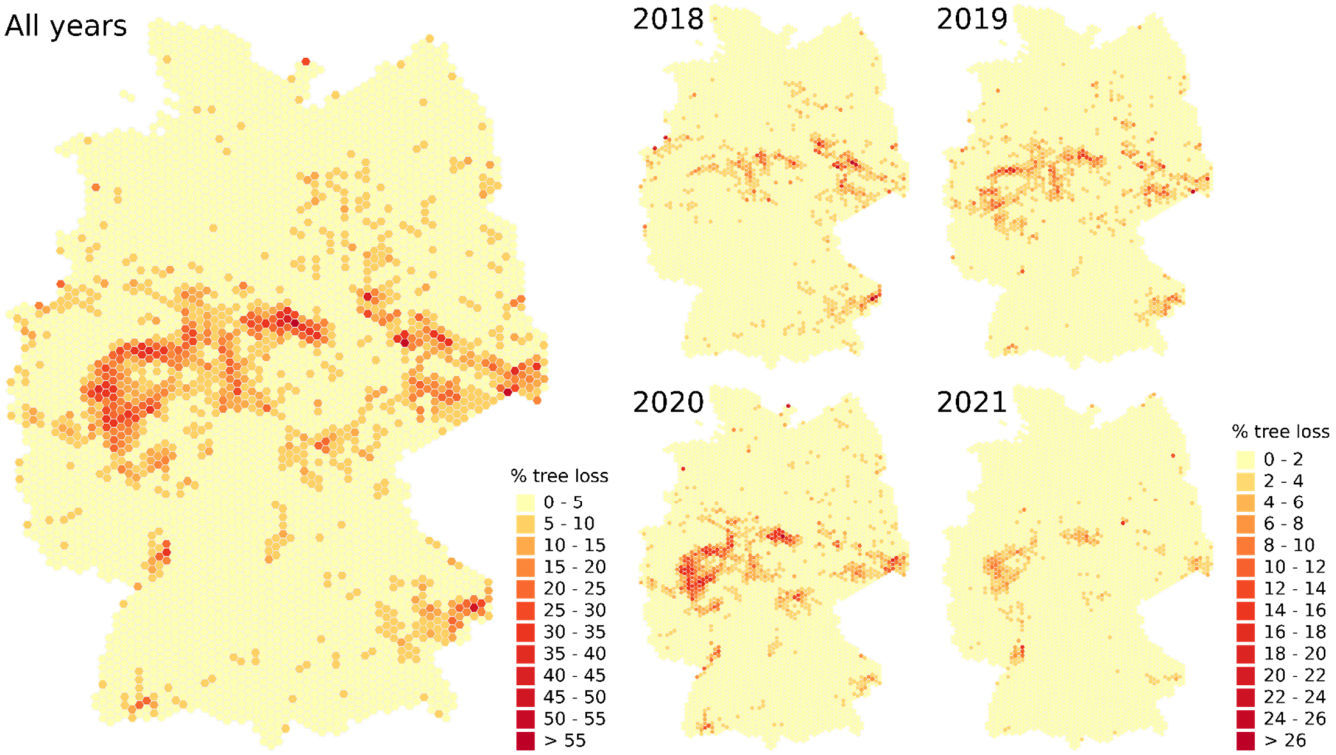

Figure 8. Forest changes (percentage loss of forest cover per hexagon) for all forest types and the period January 2018–April 2021 (left panel), 2018, 2019, 2020, and January–April 2021. Each hexagon has an area of approx. 87 km^2.

With regard to administrative levels, there are huge differences among the federal states and forest types. However, central German federal states, such as North Rhine-Westphalia, Hesse, and Saxony-Anhalt, were more affected than the northern and southern states.

Across Germany, a total of almost 9% of the coniferous trees were cleared or left standing as deadwood. In North Rhine-Westphalia, about 26% of the coniferous forests were cleared, corresponding to about 85,000 ha. Deciduous trees were less affected; they contribute to less than 1% of the forest area that was cleared in Germany. The cumulative graphs of forest loss (Figure 9) show the differences in the timing of canopy cover loss among the most affected federal states. In Bavaria, for example, the numbers rose quickly after the removal of windthrown trees and then grew steadily at relatively high rates. In North Rhine-Westphalia, clearing started to accelerate in mid-2019 and soon surpassed the rates in Bavaria, mainly driven by the removal of coniferous trees. All time series showed strong increases at the beginning of each year. This results from increased clear-cut activities in winter but could also be the effect of missing observations during winter snow or cloud cover. In this case, the winter canopy cover losses would be recorded by the presented algorithm with a short time lag as soon as the snow or cloud period ended. However, the results seem realistic as it is common practice to log trees preferably at the end of winter. The high numbers of canopy cover loss areas in early 2018 include windthrow events from late 2017. The extensive storm damage in the summer and fall of 2017 is often not reflected in the 2017 reference image because the median will level out the rise in the signal. Consequently, the majority of observations in these areas show the forest in good condition in 2017, while the first observations of 2018 record these areas as showing canopy cover loss. In terms of area, North Rhine-Westphalia, Bavaria, Hesse, Lower Saxony and Saxony-Anhalt are the most affected federal states. In terms of percentage, North Rhine-Westphalia, Saxony-Anhalt, and Saxony are most affected (Figure 9). Changes aggregated for particular years are shown in Figure 10. It can be seen that the share of coniferous forest loss is higher

than that of deciduous forests in all federal states. The loss rates increased from 2018 to 2020 in most of the federal states and are likely to still be high in 2021. Statistics of canopy cover loss per federal state can be found in the Supplementary Materials.

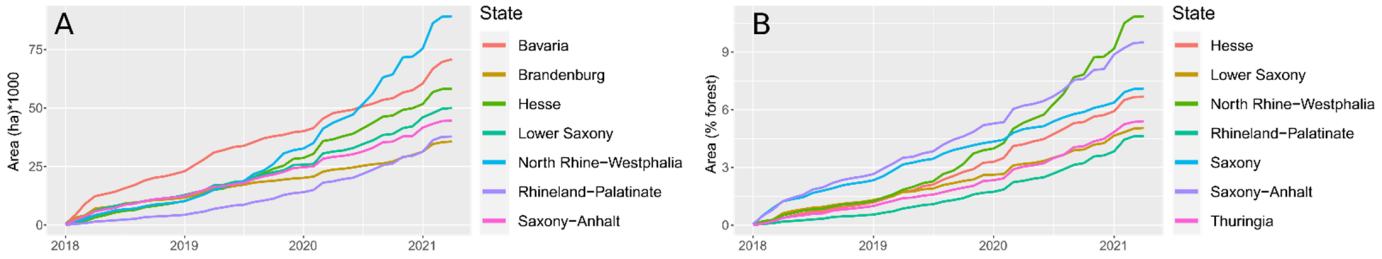

Figure 9. Canopy cover losses of the seven most affected federal states over time: (**A**) in terms of area, (**B**) in terms of percentage. Please note that the federal states differ in the two plots.

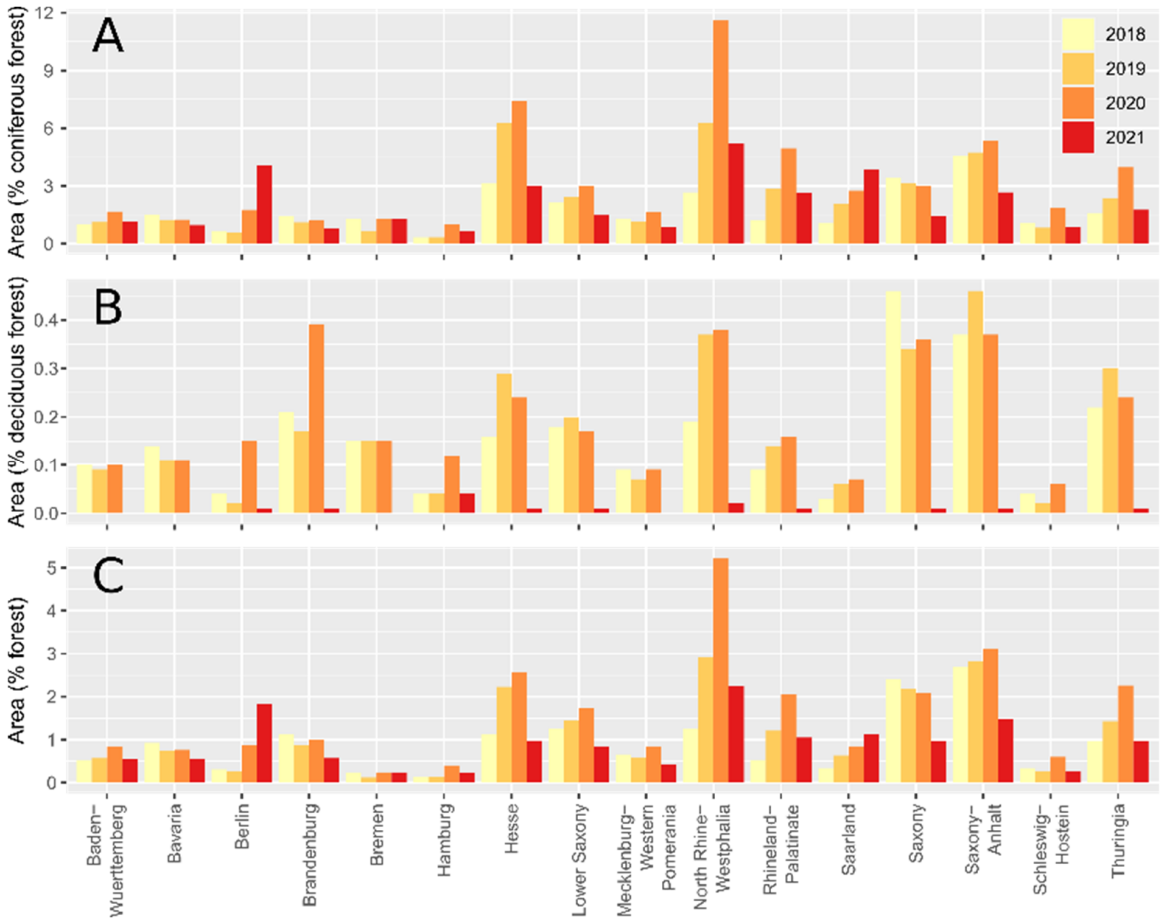

Figure 10. Canopy cover loss per federal state aggregated per year for (**A**) coniferous, (**B**) deciduous, and (**C**) all forest types.

At the district level (Landkreis), the pattern becomes clearer than at the federal state level (Figure 11). The most affected districts are located in central Germany. Some extraordinary numbers occur in districts with a very low share of one forest type, where large parts of it were cleared, translating into relatively large percentages of cleared areas (e.g., the very eastern districts of Brandenburg in Figure 11b). The annual coniferous forest loss per district is shown in Figure 12. In 2018, the districts of Göttingen (19%), Leipzig (18%) and Sömmerda (18%) had the highest percentages of coniferous canopy cover loss. Sömmerda (28%) and Soest (25%) took the lead in 2019, with Altenkirchen (Westerwald) (26%),

Oberbergischer Kreis (25%), and Westerwaldkreis (25%) catching up in 2020. Soest (27%) still had the highest coniferous forest loss rates in 2020. In absolute numbers, the districts of Harz (located in Saxony-Anhalt, 19,620 ha), Hochsauerlandkreis (North Rhine-Westphalia, 12,462 ha), Siegen-Wittgenstein (North Rhine-Westphalia, 11,794 ha), Goslar (Lower Saxony, 10,053 ha), Märkischer Kreis (North Rhine-Westphalia, 9317 ha), and Oberbergischer Kreis (North Rhine-Westphalia, 8927 ha) experienced the greatest losses of coniferous forests. These districts comprise the Harz mountain range and the Rhenish Massif, two major central German mountain ranges.

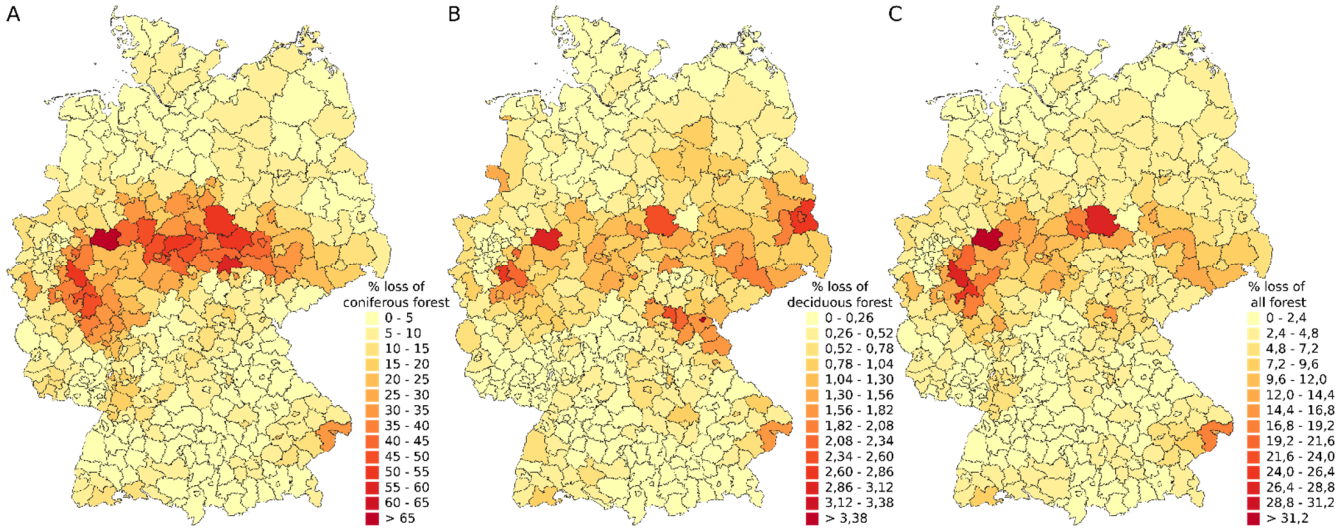

Figure 11. Canopy cover loss in coniferous forests (percentage loss of coniferous forest cover per district, (**A**), deciduous forests (percentage loss of deciduous forest cover per district, (**B**), and all forest types (**C**) for the period January 2018–April 2021.

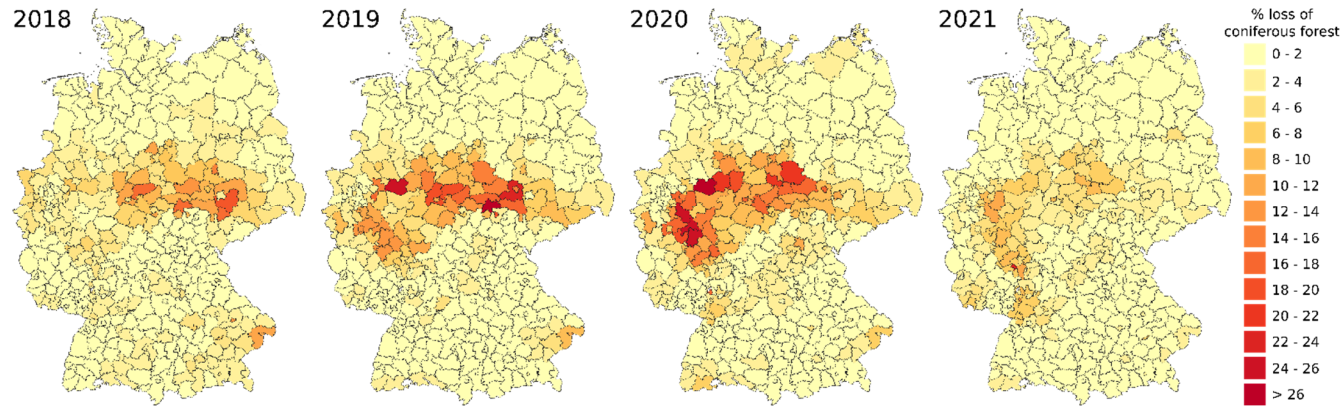

Figure 12. Loss of coniferous forest in 2018, 2019, 2020, and January–April 2021 at the district level.

Losses in deciduous forests were highest in the districts of Harz (Saxony-Anhalt, 836 ha), Hochsauerlandkreis (North Rhine-Westphalia, 544 ha), Kassel (Hesse, 507 ha), Schwalm-Eder-Kreis (Hesse, 462 ha), and Hersfeld-Rotenburg (Hesse, 442 ha). With respect to percentages, the City of Hof (Bavaria, 3.5%), and districts of Soest (North Rhine-Westphalia, 3.0%), Rheinisch-Bergischer Kreis (North Rhine-Westphalia, 2.7%), Spree-Neiße (Brandenburg, 2.6%), and Sonneberg (Thuringia, 2.5%) were most affected. The largest percentage of forest loss, regardless of forest type, was recorded for the districts of Soest (North Rhine-Westphalia, 31.6%), Harz (Saxony-Anhalt, 27.9%), Oberbergischer Kreis (North Rhine-Westphalia, 27.8%), Altenkirchen (Westerwald) (North Rhine-Westphalia, 24.7%), and Osterode am Harz (Lower Saxony, 21.0%). In absolute numbers, the districts of

Harz (Saxony-Anhalt, 20,456 ha), Hochsauerlandkreis (North Rhine-Westphalia, 13,006 ha), Siegen-Wittgenstein (North Rhine-Westphalia, 12,077 ha), Goslar (Lower Saxony, 10,231 ha), and Märkischer Kreis (North Rhine-Westphalia, 9584 ha) show the highest forest loss for all forest types.

In situations where the Copernicus forest-type layer is misclassified, the manual editing (removal of the 2020/2021 winter's canopy cover loss in deciduous forests) may cause the erroneous removal of real changes in coniferous forests or the erroneous introduction of changes in deciduous forests. Our results will therefore be improved when more accurate forest masks (actually, tree masks) and forest-type layers are available. In this study, we use a combined DLM250/Copernicus forest-type map, which limits the forest land use to the tree-covered area. Consequently, the forest coverage to which our results are related might differ from official statistics.

With regard to the spatial accuracy, our assessment based on pixel counts revealed an overall accuracy of 92.8%. The sample-based accuracy assessment [76] revealed an overall accuracy of 98% ± 1% and an area estimate of 643,735 ha ± 120,726 ha canopy cover loss (Table 2).

Table 2. Results of the accuracy assessment, based on pixel counts (left part) and based on samples (right part). PA = producer's accuracy, UA = user's accuracy, OA = overall accuracy.

	Area (ha) ("Pixel Counts")	PA	UA	OA	Estimated Area (ha)	ha±	PA	PA±	UA	UA±	OA	OA±
Canopy cover loss	501,361	0.92	0.97	0.93	643,735	120,726	0.92	0.02	0.71	0.03	0.98	0.01
Buffer	883,957	0.91	0.98		804,609	31,793	0.91	0.04	1	0.01		
Intact forest	9,376,217	0.99	0.77		9,313,191	116,467	0.99	0.01	1	0.01		

Due to the large-scale character of clear-cuts and the strong associated spectral changes, the validation of canopy cover loss is straightforward in most of the areas. Standing dead trees can also easily be identified in high-resolution data. The validation of the temporal allocation is more challenging. Within the observation period, several larger fire events took place in northern and eastern Germany, e.g., Treuenbrietzen on 23 August 2018 (Figure 7b, southern part), Lübtheen on 30 June 2019 (Figure 7c), Jüterbog on 4 June 2019 (Figure 7b, northern part), Lieberoser Heide on 26 June 2019. In our results, these fires were mapped as canopy cover loss in September 2018 (Treuenbrietzen), August 2019 (Lübtheen), July 2019 (Jüterbog) and August 2019 (Lieberoser Heide), hence, this was with only little delay.

4. Discussion

The backbone of our method is robust pre-processing and compositing to reduce outliers caused by artifacts, such as missed clouds, as much as possible. The aggregation of monthly datasets comes at the expense of temporal resolution. The monthly temporal resolution, however, is an important step toward operational monitoring and provides essential improvements compared to other available products that exist at the federal state level in Germany (e.g., quarterly or annual satellite-based assessments). Near-real-time alerting is beyond the scope of our work and would require more sophisticated methods for the identification of canopy cover loss in order to maintain accuracy. The monthly interval of our product allows the temporal allocation of canopy cover loss to the correct year with far higher accuracy than annual products. The importance of the time domain and within-year assessments of forest disturbance was demonstrated recently [77]. The authors used the time information to distinguish forest change types, which we did not intend to include in our study. The main advantage in our study—besides a more accurate temporal allocation of canopy cover loss—is that large-scale harvest and salvage logging activities often occur in winter and can thus be mapped in a more timely manner. Intra-annual mapping can be important to estimate the scale of insect outbreaks, particularly in coniferous forests [78]. We did not differentiate between regular forest harvest and additional logging in response

to drought and insect infestation. The large-scale clear-cuts that make up most of the recorded tree-loss areas should be understood as exceptional management. Consequently, most of the detected losses of the forest canopy cover result from disturbances, such as droughts and insect infestation. These are often interlinked, particularly drought and bark-beetle infestation in spruce stands [13,16]. It is worth mentioning that the canopy cover losses we recorded are not only caused by the 2018–2020 droughts and cascading effects but also include windthrow, fire and regular harvesting. Our canopy cover-loss map alone does not reveal information about the underlying causes and drivers. However, a recent study based on data between 1987 and 2016 revealed that excess forest mortality in Europe is strongly linked to drought [79]. For a complete picture, it would be useful to combine canopy cover loss records with complementary products. These could either be anomalies of spectral indices related to forest vitality [80] or climatological and other environmental data [2,81].

Compared to the annual maps provided via the global forest watch [37], our map shows generally good agreement in terms of spatial pattern. While our product shows less canopy cover loss in deciduous forests, it records much larger canopy cover loss in coniferous forests compared to the maps of the global forest watch. Other European or nationwide products in Germany do not explicitly determine canopy cover loss (e.g., [80]) and are therefore difficult to compare with our map. While national forest disturbance mapping systems were recently proposed for other Central European countries (e.g., Austria [19]), a national system does not yet exist for Germany, even though remote sensing is considered an important asset to complement ground surveys and the technology is being established at the federal state level [82–84].

Official statistics in Germany do not provide information about canopy cover loss but rather accumulate forest areas that need to be stocked because recent disturbances did not leave sufficient understory vegetation to allow for the regeneration of the forests. The area to be replanted amounts to approx. 295,000 ha [85] and is far smaller than the canopy cover loss area we estimated of 501,000 ha for about the same time frame. From the validation of our map, we see that we overestimated canopy cover loss in windthrow areas where only the affected trees were removed and, often, healthy trees were left standing, while we captured the affected area quite well. At the same time, we underestimated canopy cover loss in deciduous and mixed forests. Damages in these forest types are more challenging to assess because they are not necessarily fatal and often affect only single trees, which cannot be properly captured with the spatial resolution of Landsat and Sentinel-2.

Our method will benefit from the integration of new sensors (e.g., Landsat-9) as it will likely increase the number of available datasets.

5. Conclusions

With this article, we present a first assessment of the canopy cover loss in Germany in response to the 2018–2020 drought years. The canopy cover loss includes mainly clear-cut areas resulting from the intense sanitation and salvage logging of predominantly coniferous trees, and dead trees left standing after fires or after bark beetle infestation in spruce stands in some National Parks and also, to a minor extent, in managed forests. While a large share of canopy cover loss is caused by calamities, our results also include forest harvest. Our product has a high spatial resolution of 10 m and a high temporal resolution (monthly). The numbers we obtain are far higher than those published by the responsible agencies [85], who report areas that need to be replanted rather than areas with canopy cover loss. The canopy cover loss areas we determined include areas with live trees left standing (e.g., windthrow areas), hence, giving a good estimate of areas affected by tree mortality and forest harvest. The scope of this study is on canopy cover loss; we did not assess the processes of forest regrowth. While the processes and causes behind tree loss can be very complex, we reduced our assessment to the resultant canopy cover loss area, irrespective of the underlying causes. We used pixel counts to demonstrate regional differences and short-term trends from January 2018 to April 2021. Our accuracy assessment includes

sample-based estimates of canopy cover loss. The estimated areas are larger than those based on pixel counts. Visual inspection and quantitative accuracy assessment revealed the high quality of our results. We found that canopy cover loss rates generally increased over time throughout Germany. The hotspots of canopy cover loss are located in central Germany, and losses in coniferous forests dominate. Some districts lost more than two-thirds of their coniferous forests. Our method is based on the comprehensive removal of artifacts such as clouds and outliers and is therefore robust. Canopy cover loss can be mapped at any time. The temporal resolution allows for a more accurate allocation of canopy cover loss to the correct year. Spatially explicit information about canopy cover loss is important for the quantification of timber volumes and future forest management decisions, particularly during exceptional weather situations.

Supplementary Materials: The following are available online at https://www.mdpi.com/article/10.3390/rs14030562/s1, Table S1: Canopy cover loss per German federal state in hectares, Table S2: Canopy cover loss per German federal state in percentages.

Author Contributions: Conceptualization, F.T. and U.G.; methodology, F.T.; software, F.T.; validation, F.T. and J.K.; formal analysis, F.T.; writing—original draft preparation, F.T.; writing—review and editing, U.G., S.H., J.K., E.d.P., J.H. and C.K.; visualization, F.T.; supervision, U.G. and C.K. All authors have read and agreed to the published version of the manuscript.

Funding: This publication was supported by the open access publication fund of the German Aerospace Center (DLR).

Institutional Review Board Statement: Not applicable.

Informed Consent Statement: Not applicable.

Data Availability Statement: The canopy cover loss map produced in this study is available from the corresponding author upon reasonable request.

Acknowledgments: We are grateful for the great processing power and consistent data of the Google Earth Engine. We further thank the anonymous reviewers for their helpful comments.

Conflicts of Interest: The authors declare no conflict of interest.

References

1. Buras, A.; Rammig, A.; Zang, C.S. Quantifying Impacts of the 2018 Drought on European Ecosystems in Comparison to 2003. *Biogeosciences* **2020**, *17*, 1655–1672. [CrossRef]
2. Reinermann, S.; Gessner, U.; Asam, S.; Kuenzer, C.; Dech, S. The Effect of Droughts on Vegetation Condition in Germany: An Analysis Based on Two Decades of Satellite Earth Observation Time Series and Crop Yield Statistics. *Remote Sens.* **2019**, *11*, 1783. [CrossRef]
3. Popkin, G. Forest Fight. *Science* **2021**, *374*, 1184–1189. [CrossRef] [PubMed]
4. Philipp, M.; Wegmann, M.; Kübert-Flock, C. Quantifying the Response of German Forests to Drought Events via Satellite Imagery. *Remote Sens.* **2021**, *13*, 1845. [CrossRef]
5. Schuldt, B.; Buras, A.; Arend, M.; Vitasse, Y.; Beierkuhnlein, C.; Damm, A.; Gharun, M.; Grams, T.E.E.; Hauck, M.; Hajek, P.; et al. A First Assessment of the Impact of the Extreme 2018 Summer Drought on Central European Forests. *Basic Appl. Ecol.* **2020**, *45*, 86–103. [CrossRef]
6. *Ergebnisse der Waldzustandserhebung 2020*; BMEL: Bonn, Germany, 2021; 72p.
7. Holzwarth, S.; Thonfeld, F.; Abdullahi, S.; Asam, S.; Da Ponte Canova, E.; Gessner, U.; Huth, J.; Kraus, T.; Leutner, B.; Kuenzer, C. Earth Observation Based Monitoring of Forests in Germany: A Review. *Remote Sens.* **2020**, *12*, 3570. [CrossRef]
8. Hlásny, T.; Zimová, S.; Merganičová, K.; Štěpánek, P.; Modlinger, R.; Turčáni, M. Devastating Outbreak of Bark Beetles in the Czech Republic: Drivers, Impacts, and Management Implications. *For. Ecol. Manag.* **2021**, *490*, 119075. [CrossRef]
9. Huang, J.; Hammerbacher, A.; Weinhold, A.; Reichelt, M.; Gleixner, G.; Behrendt, T.; van Dam, N.M.; Sala, A.; Gershenzon, J.; Trumbore, S.; et al. Eyes on the Future—Evidence for Trade-Offs between Growth, Storage and Defense in Norway Spruce. *New Phytol.* **2019**, *222*, 144–158. [CrossRef]
10. Hroššo, B.; Mezei, P.; Potterf, M.; Majdák, A.; Blaženec, M.; Korolyova, N.; Jakuš, R. Drivers of Spruce Bark Beetle (Ips Typographus) Infestations on Downed Trees after Severe Windthrow. *Forests* **2020**, *11*, 1290. [CrossRef]
11. Mezei, P.; Jakuš, R.; Pennerstorfer, J.; Havašová, M.; Škvarenina, J.; Ferenčík, J.; Slivinský, J.; Bičárová, S.; Bilčík, D.; Blaženec, M.; et al. Storms, Temperature Maxima and the Eurasian Spruce Bark Beetle Ips Typographus—An Infernal Trio in Norway Spruce Forests of the Central European High Tatra Mountains. *Agric. For. Meteorol.* **2017**, *242*, 85–95. [CrossRef]

12. Stadelmann, G.; Bugmann, H.; Wermelinger, B.; Bigler, C. Spatial Interactions between Storm Damage and Subsequent Infestations by the European Spruce Bark Beetle. *For. Ecol. Manag.* **2014**, *318*, 167–174. [CrossRef]
13. Marini, L.; Økland, B.; Jönsson, A.M.; Bentz, B.; Carroll, A.; Forster, B.; Grégoire, J.-C.; Hurling, R.; Nageleisen, L.M.; Netherer, S.; et al. Climate Drivers of Bark Beetle Outbreak Dynamics in Norway Spruce Forests. *Ecography* **2017**, *40*, 1426–1435. [CrossRef]
14. Netherer, S.; Panassiti, B.; Pennerstorfer, J.; Matthews, B. Acute Drought Is an Important Driver of Bark Beetle Infestation in Austrian Norway Spruce Stands. *Front. For. Glob. Chang.* **2019**, *2*, 39. [CrossRef]
15. Seidl, R.; Thom, D.; Kautz, M.; Martin-Benito, D.; Peltoniemi, M.; Vacchiano, G.; Wild, J.; Ascoli, D.; Petr, M.; Honkaniemi, J.; et al. Forest Disturbances under Climate Change. *Nat. Clim. Chang.* **2017**, *7*, 395–402. [CrossRef]
16. Hlásny, T.; König, L.; Krokene, P.; Lindner, M.; Montagné-Huck, C.; Müller, J.; Qin, H.; Raffa, K.F.; Schelhaas, M.-J.; Svoboda, M.; et al. Bark Beetle Outbreaks in Europe: State of Knowledge and Ways Forward for Management. *Curr. For. Rep.* **2021**, *7*, 138–165. [CrossRef]
17. Hlásny, T.; Krokene, P.; Liebhold, A.; Montagné-Huck, C.; Müller, J.; Qin, H.; Raffa, K.; Schelhaas, M.-J.; Seidl, R.; Svoboda, M.; et al. *Living with Bark Beetles: Impacts, Outlook and Management Options*; European Forest Institute: Joensuu, Finland, 2019.
18. Fernandez-Carrillo, A.; Patočka, Z.; Dobrovolný, L.; Franco-Nieto, A.; Revilla-Romero, B. Monitoring Bark Beetle Forest Damage in Central Europe. A Remote Sensing Approach Validated with Field Data. *Remote Sens.* **2020**, *12*, 3634. [CrossRef]
19. Löw, M.; Koukal, T. Phenology Modelling and Forest Disturbance Mapping with Sentinel-2 Time Series in Austria. *Remote Sens.* **2020**, *12*, 4191. [CrossRef]
20. Statistisches Bundesamt (Destatis) Forest Damage: Logging of Timber Damaged by Insect Infestation Grew More than Tenfold within Five Years. Available online: https://www.destatis.de/EN/Press/2021/08/PE21_N050_41.html;jsessionid=63F86D4A9948D3E9015C6FF57C3994A0.live712 (accessed on 10 December 2021).
21. *Waldbericht der Bundesregierung 2021*; BMEL: Bonn, Germany, 2021; 84p.
22. Sandström, J.; Bernes, C.; Junninen, K.; Lõhmus, A.; Macdonald, E.; Müller, J.; Jonsson, B.G. Impacts of Dead Wood Manipulation on the Biodiversity of Temperate and Boreal Forests. A Systematic Review. *J. Appl. Ecol.* **2019**, *56*, 1770–1781. [CrossRef]
23. De Rigo, D.; Bosco, C.; San-Miguel-Ayanz, J.; Durrant, T.; Barredo Cano, J.I.; Strona, G.; Caudullo, G.; Di Leo, M.; Boca, R. *Forest Resources in Europe: An Integrated Perspective on Ecosystem Services, Disturbances and Threats. European Atlas of Forest Tree Species*; Publication Office of the European Union: Brussels, Belgium, 2016; ISBN 978-92-79-52833-0.
24. Banskota, A.; Kayastha, N.; Falkowski, M.J.; Wulder, M.A.; Froese, R.E.; White, J.C. Forest Monitoring Using Landsat Time Series Data: A Review. *Can. J. Remote Sens.* **2014**, *40*, 362–384. [CrossRef]
25. Hermosilla, T.; Wulder, M.A.; White, J.C.; Coops, N.C.; Hobart, G.W. Regional Detection, Characterization, and Attribution of Annual Forest Change from 1984 to 2012 Using Landsat-Derived Time-Series Metrics. *Remote Sens. Environ.* **2015**, *170*, 121–132. [CrossRef]
26. Kennedy, R.E.; Yang, Z.; Cohen, W.B. Detecting Trends in Forest Disturbance and Recovery Using Yearly Landsat Time Series: 1. LandTrendr—Temporal Segmentation Algorithms. *Remote Sens. Environ.* **2010**, *114*, 2897–2910. [CrossRef]
27. Schroeder, T.A.; Wulder, M.A.; Healey, S.P.; Moisen, G.G. Mapping Wildfire and Clearcut Harvest Disturbances in Boreal Forests with Landsat Time Series Data. *Remote Sens. Environ.* **2011**, *115*, 1421–1433. [CrossRef]
28. White, J.C.; Wulder, M.A.; Hermosilla, T.; Coops, N.C.; Hobart, G.W. A Nationwide Annual Characterization of 25 Years of Forest Disturbance and Recovery for Canada Using Landsat Time Series. *Remote Sens. Environ.* **2017**, *194*, 303–321. [CrossRef]
29. Wulder, M.A.; Hermosilla, T.; Stinson, G.; Gougeon, F.A.; White, J.C.; Hill, D.A.; Smiley, B.P. Satellite-Based Time Series Land Cover and Change Information to Map Forest Area Consistent with National and International Reporting Requirements. *For. Int. J. For. Res.* **2020**, *93*, 331–343. [CrossRef]
30. Hansen, M.C.; Krylov, A.; Tyukavina, A.; Potapov, P.V.; Turubanova, S.; Zutta, B.; Ifo, S.; Margono, B.; Stolle, F.; Moore, R. Humid Tropical Forest Disturbance Alerts Using Landsat Data. *Environ. Res. Lett.* **2016**, *11*, 034008. [CrossRef]
31. Reiche, J.; Mullissa, A.; Slagter, B.; Gou, Y.; Tsendbazar, N.-E.; Odongo-Braun, C.; Vollrath, A.; Weisse, M.J.; Stolle, F.; Pickens, A.; et al. Forest Disturbance Alerts for the Congo Basin Using Sentinel-1. *Environ. Res. Lett.* **2021**, *16*, 024005. [CrossRef]
32. Scharvogel, D.; Brandmeier, M.; Weis, M. A Deep Learning Approach for Calamity Assessment Using Sentinel-2 Data. *Forests* **2020**, *11*, 1239. [CrossRef]
33. Bárta, V.; Lukeš, P.; Homolová, L. Early Detection of Bark Beetle Infestation in Norway Spruce Forests of Central Europe Using Sentinel-2. *Int. J. Appl. Earth Obs. Geoinformation* **2021**, *100*, 102335. [CrossRef]
34. Huo, L.; Persson, H.J.; Lindberg, E. Early Detection of Forest Stress from European Spruce Bark Beetle Attack, and a New Vegetation Index: Normalized Distance Red & SWIR (NDRS). *Remote Sens. Environ.* **2021**, *255*, 112240. [CrossRef]
35. Pasquarella, V.J.; Bradley, B.A.; Woodcock, C.E. Near-Real-Time Monitoring of Insect Defoliation Using Landsat Time Series. *Forests* **2017**, *8*, 275. [CrossRef]
36. San-Miguel-Ayanz, J.; Durrant, T.; Boca, R.; Maianti, P.; Libertá, G.; Artés-Vivancos, T.; Oom, D.; Branco, A.; De Rigo, D.; Ferrari, D.; et al. *Advance EFFIS Report on Forest Fires in Europe, Middle East and North Africa 2020, EUR 30693EN.*; Publications Office of the European Union: Luxembourg, 2021.
37. Hansen, M.C.; Potapov, P.V.; Moore, R.; Hancher, M.; Turubanova, S.A.; Tyukavina, A.; Thau, D.; Stehman, S.V.; Goetz, S.J.; Loveland, T.R.; et al. High-Resolution Global Maps of 21st-Century Forest Cover Change. *Science* **2013**, *342*, 850–853. [CrossRef]
38. Frantz, D. FORCE—Landsat + Sentinel-2 Analysis Ready Data and Beyond. *Remote Sens.* **2019**, *11*, 1124. [CrossRef]

39. Griffiths, P.; van der Linden, S.; Kuemmerle, T.; Hostert, P. A Pixel-Based Landsat Compositing Algorithm for Large Area Land Cover Mapping. *IEEE J. Sel. Top. Appl. Earth Obs. Remote Sens.* **2013**, *6*, 2088–2101. [CrossRef]
40. White, J.C.; Wulder, M.A.; Hobart, G.W.; Luther, J.E.; Hermosilla, T.; Griffiths, P.; Coops, N.C.; Hall, R.J.; Hostert, P.; Dyk, A.; et al. Pixel-Based Image Compositing for Large-Area Dense Time Series Applications and Science. *Can. J. Remote Sens.* **2014**, *40*, 192–212. [CrossRef]
41. Mack, B.; Leinenkugel, P.; Kuenzer, C.; Dech, S. A Semi-Automated Approach for the Generation of a New Land Use and Land Cover Product for Germany Based on Landsat Time-Series and Lucas *in-Situ* Data. *Remote Sens. Lett.* **2017**, *8*, 244–253. [CrossRef]
42. Müller, H.; Rufin, P.; Griffiths, P.; Barros Siqueira, A.J.; Hostert, P. Mining Dense Landsat Time Series for Separating Cropland and Pasture in a Heterogeneous Brazilian Savanna Landscape. *Remote Sens. Environ.* **2015**, *156*, 490–499. [CrossRef]
43. Thonfeld, F.; Steinbach, S.; Muro, J.; Kirimi, F. Long-Term Land Use/Land Cover Change Assessment of the Kilombero Catchment in Tanzania Using Random Forest Classification and Robust Change Vector Analysis. *Remote Sens.* **2020**, *12*, 1057. [CrossRef]
44. Abdullah, H.; Darvishzadeh, R.; Skidmore, A.K.; Heurich, M. Sensitivity of Landsat-8 OLI and TIRS Data to Foliar Properties of Early Stage Bark Beetle (Ips Typographus, L.) Infestation. *Remote Sens.* **2019**, *11*, 398. [CrossRef]
45. Abdullah, H.; Darvishzadeh, R.; Skidmore, A.K.; Groen, T.A.; Heurich, M. European Spruce Bark Beetle (Ips Typographus, L.) Green Attack Affects Foliar Reflectance and Biochemical Properties. *Int. J. Appl. Earth Obs. Geoinform.* **2018**, *64*, 199–209. [CrossRef]
46. Einzmann, K.; Immitzer, M.; Böck, S.; Bauer, O.; Schmitt, A.; Atzberger, C. Windthrow Detection in European Forests with Very High-Resolution Optical Data. *Forests* **2017**, *8*, 21. [CrossRef]
47. Tanase, M.A.; Aponte, C.; Mermoz, S.; Bouvet, A.; Le Toan, T.; Heurich, M. Detection of Windthrows and Insect Outbreaks by L-Band SAR: A Case Study in the Bavarian Forest National Park. *Remote Sens. Environ.* **2018**, *209*, 700–711. [CrossRef]
48. Forzieri, G.; Girardello, M.; Ceccherini, G.; Spinoni, J.; Feyen, L.; Hartmann, H.; Beck, P.S.A.; Camps-Valls, G.; Chirici, G.; Mauri, A.; et al. Emergent Vulnerability to Climate-Driven Disturbances in European Forests. *Nat. Commun.* **2021**, *12*, 1081. [CrossRef] [PubMed]
49. Senf, C.; Pflugmacher, D.; Zhiqiang, Y.; Sebald, J.; Knorn, J.; Neumann, M.; Hostert, P.; Seidl, R. Canopy Mortality Has Doubled in Europe's Temperate Forests over the Last Three Decades. *Nat. Commun.* **2018**, *9*, 4978. [CrossRef] [PubMed]
50. Senf, C.; Seidl, R. Mapping the Forest Disturbance Regimes of Europe. *Nat. Sustain.* **2021**, *4*, 63–70. [CrossRef]
51. Wellbrock, N.; Bolte, A. (Eds.) *Status and Dynamics of Forests in Germany: Results of the National Forest Monitoring*; Ecological Studies; Springer Open: Berlin/Heidelberg, Germany, 2019; ISBN 978-3-030-15732-6.
52. Healey, S.; Cohen, W.; Zhiqiang, Y.; Krankina, O. Comparison of Tasseled Cap-Based Landsat Data Structures for Use in Forest Disturbance Detection. *Remote Sens. Environ.* **2005**, *97*, 301–310. [CrossRef]
53. Gorelick, N.; Hancher, M.; Dixon, M.; Ilyushchenko, S.; Thau, D.; Moore, R. Google Earth Engine: Planetary-Scale Geospatial Analysis for Everyone. *Remote Sens. Environ.* **2017**, *202*, 18–27. [CrossRef]
54. Qiu, S.; Zhu, Z.; Shang, R.; Crawford, C.J. Can Landsat 7 Preserve Its Science Capability with a Drifting Orbit? *Sci. Remote Sens.* **2021**, *4*, 100026. [CrossRef]
55. Markham, B.L.; Storey, J.C.; Williams, D.L.; Irons, J.R. Landsat Sensor Performance: History and Current Status. *IEEE Trans. Geosci. Remote Sens.* **2004**, *42*, 2691–2694. [CrossRef]
56. Mueller-Wilm, U.; Devignot, O.; Pessiot, L. S2 MPC—Sen2Cor Configuration and User Manual, Ref. S2-PDGS-MPC-L2A-SUM-V2.9, Issue 1. 2020. Available online: http://step.esa.int/thirdparties/sen2cor/2.9.0/docs/S2-PDGS-MPC-L2A-SUM-V2.9.0.pdf (accessed on 10 December 2021).
57. Vermote, E.; Roger, J.C.; Franch, B.; Skakun, S. LaSRC (Land Surface Reflectance Code): Overview, Application and Validation Using MODIS, VIIRS, LANDSAT and Sentinel 2 Data's. In Proceedings of the IGARSS 2018—2018 IEEE International Geoscience and Remote Sensing Symposium, Valencia, Spain, 22–27 July 2018; pp. 8173–8176.
58. Frantz, D.; Haß, E.; Uhl, A.; Stoffels, J.; Hill, J. Improvement of the Fmask Algorithm for Sentinel-2 Images: Separating Clouds from Bright Surfaces Based on Parallax Effects. *Remote Sens. Environ.* **2018**, *215*, 471–481. [CrossRef]
59. Zhu, Z.; Wang, S.; Woodcock, C.E. Improvement and Expansion of the Fmask Algorithm: Cloud, Cloud Shadow, and Snow Detection for Landsats 4–7, 8, and Sentinel 2 Images. *Remote Sens. Environ.* **2015**, *159*, 269–277. [CrossRef]
60. Zhu, Z.; Woodcock, C.E. Object-Based Cloud and Cloud Shadow Detection in Landsat Imagery. *Remote Sens. Environ.* **2012**, *118*, 83–94. [CrossRef]
61. Hall, D.K.; Riggs, G.A.; Salomonson, V.V. Development of Methods for Mapping Global Snow Cover Using Moderate Resolution Imaging Spectroradiometer Data. *Remote Sens. Environ.* **1995**, *54*, 127–140. [CrossRef]
62. Shimamura, Y.; Izumi, T.; Matsuyama, H. Evaluation of a Useful Method to Identify Snow-covered Areas under Vegetation—Comparisons among a Newly Proposed Snow Index, Normalized Difference Snow Index, and Visible Reflectance. *Int. J. Remote Sens.* **2006**, *27*, 4867–4884. [CrossRef]
63. Tucker, C.J. Red and Photographic Infrared Linear Combinations for Monitoring Vegetation. *Remote Sens. Environ.* **1979**, *8*, 127–150. [CrossRef]
64. Crist, E.P.; Cicone, R.C. A Physically-Based Transformation of Thematic Mapper Data—The TM Tasseled Cap. *IEEE Trans. Geosci. Remote Sens.* **1984**, *GE-22*, 256–263. [CrossRef]

65. Kauth, R.J.; Thomas, G.S. The Tasselled Cap—A Graphic Description of the Spectral-Temporal Development of Agricultural Crops as Seen by LANDSAT. In *Symposium on Machine Processing of Remotely Sensed Data*; Purdue University: West Lafayette IN, USA, 1976; p. 13.
66. Crist, E.P. A TM Tasseled Cap Equivalent Transformation for Reflectance Factor Data. *Remote Sens. Environ.* **1985**, *17*, 301–306. [CrossRef]
67. GeoBasis-DE/BKG Digitales Landschaftsmodell 1:250000 (DLM250). 2020. Available online: http://gdz.bkg.bund.de/index.php/default/digitales-landschaftsmodell-1-250-000-ebenen-dlm250-ebenen.html (accessed on 10 December 2021).
68. European Environment Agency (EEA). *Forest Type 2015*; EEA: Copenhagen, Denmark, 2017.
69. Thonfeld, F. The Impact of Sensor Characteristics and Data Availability on Remote Sensing Based Change Detection. Ph.D. Thesis, Friedrich Wilhelms Universität, Bonn, Germany, 2014.
70. Olofsson, P.; Arévalo, P.; Espejo, A.B.; Green, C.; Lindquist, E.; McRoberts, R.E.; Sanz, M.J. Mitigating the Effects of Omission Errors on Area and Area Change Estimates. *Remote Sens. Environ.* **2020**, *236*, 111492. [CrossRef]
71. Hartmann, H.; Moura, C.F.; Anderegg, W.R.L.; Ruehr, N.K.; Salmon, Y.; Allen, C.D.; Arndt, S.K.; Breshears, D.D.; Davi, H.; Galbraith, D.; et al. Research Frontiers for Improving Our Understanding of Drought-induced Tree and Forest Mortality. *New Phytol.* **2018**, *218*, 15–28. [CrossRef]
72. Hart, S.J.; Veblen, T.T. Detection of Spruce Beetle-Induced Tree Mortality Using High- and Medium-Resolution Remotely Sensed Imagery. *Remote Sens. Environ.* **2015**, *168*, 134–145. [CrossRef]
73. Adams, H.D.; Zeppel, M.J.B.; Anderegg, W.R.L.; Hartmann, H.; Landhäusser, S.M.; Tissue, D.T.; Huxman, T.E.; Hudson, P.J.; Franz, T.E.; Allen, C.D.; et al. A Multi-Species Synthesis of Physiological Mechanisms in Drought-Induced Tree Mortality. *Nat. Ecol. Evol.* **2017**, *1*, 1285–1291. [CrossRef] [PubMed]
74. Arend, M.; Link, R.M.; Patthey, R.; Hoch, G.; Schuldt, B.; Kahmen, A. Rapid Hydraulic Collapse as Cause of Drought-Induced Mortality in Conifers. *Proc. Natl. Acad. Sci. USA* **2021**, *118*, e2025251118. [CrossRef] [PubMed]
75. Obladen, N.; Dechering, P.; Skiadaresis, G.; Tegel, W.; Keßler, J.; Höllerl, S.; Kaps, S.; Hertel, M.; Dulamsuren, C.; Seifert, T.; et al. Tree Mortality of European Beech and Norway Spruce Induced by 2018-2019 Hot Droughts in Central Germany. *Agric. For. Meteorol.* **2021**, *307*, 108482. [CrossRef]
76. Olofsson, P.; Foody, G.M.; Herold, M.; Stehman, S.V.; Woodcock, C.E.; Wulder, M.A. Good Practices for Estimating Area and Assessing Accuracy of Land Change. *Remote Sens. Environ.* **2014**, *148*, 42–57. [CrossRef]
77. Cardille, J.A.; Perez, E.; Crowley, M.A.; Wulder, M.A.; White, J.C.; Hermosilla, T. Multi-Sensor Change Detection for within-Year Capture and Labelling of Forest Disturbance. *Remote Sens. Environ.* **2022**, *268*, 112741. [CrossRef]
78. Stereńczak, K.; Mielcarek, M.; Modzelewska, A.; Kraszewski, B.; Fassnacht, F.E.; Hilszczański, J. Intra-Annual Ips Typographus Outbreak Monitoring Using a Multi-Temporal GIS Analysis Based on Hyperspectral and ALS Data in the Białowieża Forests. *For. Ecol. Manag.* **2019**, *442*, 105–116. [CrossRef]
79. Senf, C.; Buras, A.; Zang, C.S.; Rammig, A.; Seidl, R. Excess Forest Mortality Is Consistently Linked to Drought across Europe. *Nat. Commun.* **2020**, *11*, 6200. [CrossRef]
80. Buras, A.; Rammig, A.; Zang, C.S. The European Forest Condition Monitor: Using Remotely Sensed Forest Greenness to Identify Hot Spots of Forest Decline. *Front. Plant Sci.* **2021**, *12*, 689220. [CrossRef]
81. Brun, P.; Psomas, A.; Ginzler, C.; Thuiller, W.; Zappa, M.; Zimmermann, N.E. Large-Scale Early-Wilting Response of Central European Forests to the 2018 Extreme Drought. *Glob. Chang. Biol.* **2020**, *26*, 7021–7035. [CrossRef]
82. Ackermann, J.; Adler, P.; Engels, F.; Hoffmann, K.; Jütte, K.; Rüffer, O.; Sagischewski, H.; Seitz, R. Forstliche Fernerkundung in den Bundesländern auf neuen Wegen. *AFZ-DerWald* **2014**, *9*, 8–10.
83. Nink, S.; Hill, J.; Stoffels, J.; Buddenbaum, H.; Frantz, D.; Langshausen, J. Using Landsat and Sentinel-2 Data for the Generation of Continuously Updated Forest Type Information Layers in a Cross-Border Region. *Remote Sens.* **2019**, *11*, 2337. [CrossRef]
84. Stoffels, J.; Hill, J.; Sachtleber, T.; Mader, S.; Buddenbaum, H.; Stern, O.; Langshausen, J.; Dietz, J.; Ontrup, G. Satellite-Based Derivation of High-Resolution Forest Information Layers for Operational Forest Management. *Forests* **2015**, *6*, 1982–2013. [CrossRef]
85. *Zahlen & Fakten Zum Waldgipfel Am 2. Juni 2021*; BMEL: Bonn, Germany, 2021.